Beta Sheets with a Twist: The Conformation of Helical Polyisocyanopeptides Determined by Using Vibrational Circular Dichroism

ARTICLE *in* CHEMISTRY - A EUROPEAN JOURNAL · SEPTEMBER 2013

Impact Factor: 5.73 · DOI: 10.1002/chem.201300073 · Source: PubMed

11 AUTHORS, INCLUDING:

Patrick Brocorens
Université de Mons
30 PUBLICATIONS **593** CITATIONS
SEE PROFILE

David Beljonne
Université de Mons
355 PUBLICATIONS **15,301** CITATIONS
SEE PROFILE

Sander Woutersen
University of Amsterdam
103 PUBLICATIONS **4,303** CITATIONS
SEE PROFILE

Benoît Champagne
University of Namur
401 PUBLICATIONS **8,753** CITATIONS
SEE PROFILE

CHEMISTRY
A EUROPEAN JOURNAL

ChemPubSoc
Europe

DOI: 10.1002/chem.201300073

Beta Sheets with a Twist: The Conformation of Helical Polyisocyanopeptides Determined by Using Vibrational Circular Dichroism

Erik Schwartz,[a] Vincent Liégeois,[b] Matthieu Koepf,[a] Pavol Bodis,[c] Jeroen J. L. M. Cornelissen,[d] Patrick Brocorens,[e] David Beljonne,[e] Roeland J. M. Nolte,*[a] Alan E. Rowan,*[a] Sander Woutersen,*[c] and Benoît Champagne*[b]

Abstract: Detailed information on the architecture of polyisocyanopeptides based on vibrational circular dichroism (VCD) spectroscopy in combination with DFT calculations is presented. It is demonstrated that the screw sense of the helical polyisocyanides can be determined directly from the C=N-stretch vibrational region of the VCD spectrum. Analysis of the VCD signals associated with the amide I and amide II modes provides detailed information on the peptide side-chain arrangement in the polymer and indicates the presence of a helical β-sheet architecture, in which the dihedral angles are slightly different to those of natural β-sheet helices.

Keywords: density functional calculations · helical structures · hydrogen bonding · polyisocyanides · vibrational circular dichroism

Introduction

In the course of evolution, nature has developed a great variety of biomacromolecules that rely on their unique three-dimensional structure to perform specific tasks and functions. This ingenuity of nature in successfully tailoring unique (macro)molecular architectures has inspired scientists in many different research fields to develop synthetic molecular architectures featuring structural elements similar to those in the biological counterparts.[1] In particular, helix formation has received considerable attention, because in synthetic helical polymers, as in naturally occurring helical polymers, correlations have been found between the chemical and physical properties and the conformations of the macromolecular backbones.[2] Polyisocyanides[3] are helical polymers that possess the unusual feature that every carbon atom of the main chain bears a substituent. This particularity results in considerable steric hindrance and, therefore, restricted rotation around the carbon atoms of the polymer backbone. To minimize the steric hindrance, the C–C bonds twist and the backbone adopts a helical structure. Millich proposed the so-called four-over-one helix, denoted as 4_1 (that is, four repeat units per helical turn), for the main carbon chain in polyisocyanides.[3a] Experimental evidence for helical folding was provided by the resolution of poly((*tert*)-butylisocyanide), which contains achiral side chains, into two optical antipodes by using chiral column chromatography.[4] Since then, a vast number of polyisocyanides have been prepared, by using chiral monomers or chiral catalysts to promote the formation of an excess of either left-handed (*M*) or right-handed (*P*) helices.[5] The helical conformation of polyisocyanides is only stable if the side chains are sufficiently bulky. The introduction of a chiral peptide unit (for example, derived from L- and/or D-alanine) as a side chain gives further stabilization of the helical structure through the formation of hydrogen bonds between the peptide amide groups;[6] moreover, the formation of an extended hydrogen-bonding network in these polymers results in very stiff polymer chains.[7] In the case of alanylalanine-derived polyisocyanopeptides (PIAAs), infrared and ^{1}H NMR spectroscopic investigations demonstrated that the hydro-

[a] Dr. E. Schwartz,[+] Dr. M. Koepf, Prof. Dr. R. J. M. Nolte, Prof. Dr. A. E. Rowan
Radboud University Nijmegen, Institute for Molecules and Materials
Toernooiveld 1, 6525ED Nijmegen (The Netherlands)
E-mail: r.nolte@science.ru.nl
a.rowan@science.ru.nl

[b] Dr. V. Liégeois,[+] Prof. Dr. B. Champagne
Laboratoire de Chimie Théorique (LCT)
Unité de Chimie Physique Théorique et Structurale
University of Namur (UNamur)
Rue de Bruxelles, 61, 5000 Namur (Belgium)
E-mail: benoit.champagne@unamur.be

[c] Dr. P. Bodis, Dr. S. Woutersen
Van't Hoff Institute for Molecular Sciences
University of Amsterdam, Science Park 904
1098XH Amsterdam (The Netherlands)
E-mail: s.woutersen@uva.nl

[d] Prof. Dr. J. J. L. M. Cornelissen
Laboratory for Biomolecular Nanotechnology, MESA + Institute
University of Twente, Enschede (The Netherlands)

[e] Dr. P. Brocorens, Dr. D. Beljonne
Université de Mons, Place du Parc 20, 7000 Mons (Belgium)

[+] These authors contributed equally to this work.

Supporting information for this article is available on the WWW under http://dx.doi.org/10.1002/chem.201300073.

gen-bonding arrangement is preserved in solution.[8] Although initial infrared studies suggest a conformation in which the side chains adopt a helical β-sheet-like architecture, details of the conformation remain unclear, despite the fact that a range of spectroscopic techniques has been applied to these polymers.[9] To investigate the conformation of PIAAs in greater detail, we have focused our attention on vibrational circular dichroism (VCD) spectroscopy. This technique,[10] which is the extension of electronic CD (ECD) spectroscopy to vibrational transitions, has emerged as a powerful method to investigate the conformation of chiral molecules due to the rich structure information that it provides. Historically, the majority of VCD studies were aimed at the determination of the stereoconformational properties of small chiral compounds,[11] but a growing area of applications involves larger molecular architectures, such as (oligo)-peptides,[12] DNA and proteins,[13] foldamers,[14] supramolecular assemblies,[15] nanoparticles and chiral (metal) complexes,[16] and polymers.[17] Herein, we report the successful elucidation of the structure of a PIAA by using a combination of VCD spectroscopy and ab initio calculations. Similarly to VCD studies on peptides and proteins, we direct our attention to the amide I and amide II vibrational modes as the regions that are structurally the most sensitive,[18] in order to investigate the conformation of PIAA.

Results and Discussion

The helical polyisocyanopeptides **1a** (poly(isocyano-D-alanyl-L-alanine methyl ester)) and **1b** (poly(isocyano-L-alanyl-D-alanine methyl ester); Figure 1 A) were synthesized according to previously reported methods.[6] The UV/CD spectra of **1** have been discussed in detail previously,[6,19] and it is well established that the well-defined arrangement of the amide groups, as a result of the intramolecular hydrogen bonding, makes a major contribution to the Cotton effect at $\lambda = 310$ nm observed in the CD spectra (Figure 1 C). A schematic drawing of the polyisocyanide, in which the arrows represent the peptide chains that run parallel to the helical polymer axis, is shown in Figure 1 B. Previously, we determined the screw sense of poly((*R*)-2-isocyanooctane) and its enantiomer by making use of a semiquantitative coupled-oscillator approach to interpret the VCD response of the backbone imine C=N-stretching mode.[20] Based on these results, the screw sense of **1** can be determined directly from the sign of the couplet associated with the imine C=N-stretch VCD signature, observed between 1600 and 1640 cm^{-1}, without any need for additional calculations. As shown in Figure 2, we find that the C=N-stretch mode in the VCD spectrum of **1a**, for which a left-handed (*M*) helix was *indirectly* assigned by using an azo dye as a spectator group,[9a] resembles the C=N stretch observed in the VCD spectrum of poly((*R*)-2-isocyanooctane) (Figure S1 in the Supporting Information), for which a left-handed (*M*) helix was *directly* assigned by using the coupled-oscillator approximation; hence, the initial assignment was correct and **1a** is

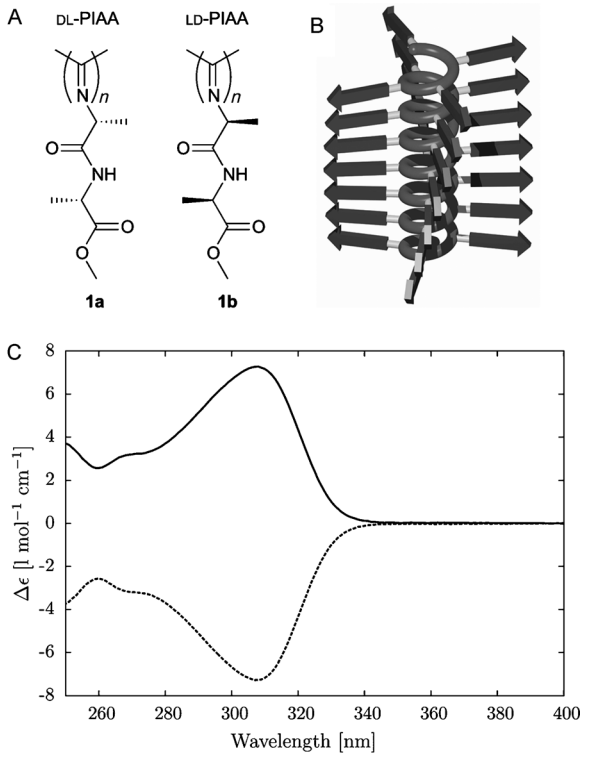

Figure 1. A) Molecular structure of polyisocyanides **1**, derived from alanylalanine. B) Schematic drawing of PIAA. C) UV/CD spectra of **1a** (dotted line) and **1b** (solid line) in $CHCl_3$.

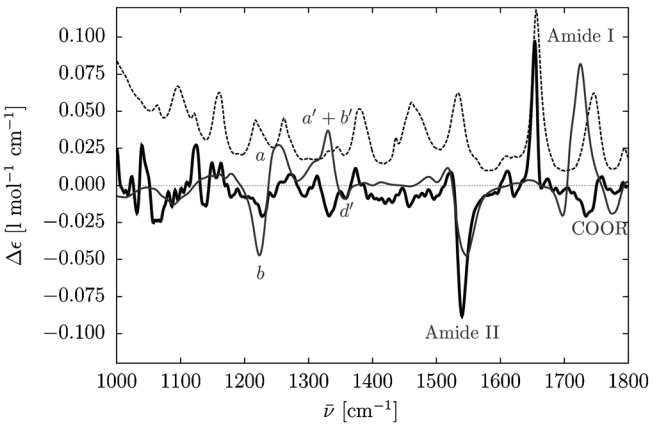

Figure 2. VCD spectra of **1b** (black thick line) and absorbance (ε/8000, dashed line) of **1b** in $CDCl_3$ (80 mM; pathlength = 0.1 mm). The VCD spectra have been corrected by subtracting the average of the **1a** and **1b** VCD intensities (see the Experimental Section). The simulated B3LYP/6-31G* VCD spectra ($\Delta\varepsilon$/10, thin line) of the most stable conformer of the 14-unit chain of **1b** is also shown.

a left-handed (*M*) helix. Analogously, a right-handed (*P*) helix can be assigned for **1b**. However, the coupled-oscillator approach cannot be used to derive the conformation of the H-bonded peptide side chains from the amide I and amide II region of the VCD spectra of **1**, because nonsymmetrical couplets, that is, nonequal and opposite VCD contributions, are observed. We thus ventured to elucidate the complete (backbone and peptide side-chain) conformation of **1**

by using DFT calculations to interpret the VCD spectrum. To obtain the initial geometrical structures, we started with an LD-PIAA polymer chain of 60 units, the structure of which was initially optimized by using a modified Dreiding force field[5i] and was further refined by using DFT and the Gaussian 09 program (see the Experimental Section).[21] From this optimized structure, segments of 8 and 14 repeating units were extracted and further optimized with DFT. The refined structures of the 8-mer and 14-mer are consistent with the initial 60-mer structure.

As can be seen from Figure 2, the amide I and amide II modes are the most pronounced signals in the VCD spectrum, and we directed our attention to these modes to investigate the structure of the PIAA. Nevertheless, the origins of the other signatures will also be described briefly. The simulated IR and VCD spectra for two chain lengths (8 and 14 repeating units) and two exchange-correlation functionals (that is, B3LYP and ωB97X-D with the 6-31G* basis set; see the Experimental Section) are shown in Figure 3. Enlargement of the chain globally improves the agreement between the simulated and measured spectra, particularly for the VCD signature at around 1540 cm^{-1}, which changes from a bisignate feature in the 8-unit chain to an almost negative peak for the 14-unit chain. The choice of exchange-correlation functional also has a small influence on the spectral features. Additional calculations were carried out 1) on the eight-unit chain by using the 6-311G* basis set (instead of 6-31G*) and 2) to account for the effects of the solvent within the polarizable continuum model (Figure S2 in the Supporting Information); these calculations confirm, and even improve, the agreement with the experimental spectrum. The 1500–1800 cm^{-1} region is characterized by normal modes with three kinds of atomic displacements. The 1500–1600 cm^{-1} zone corresponds to the amide II region with N–H bending and C–N and C^{α}–N stretching motions. The 1700–1750 cm^{-1} region forms the amide I band and consists of C=O-stretching and N–H- and C^{α}–H-bending modes. The last zone, ranging from 1750–1800 cm^{-1}, is associated with the C=O stretching of the terminal ester groups. Each of the three regions/bands is composed of the 8 (14) normal modes for the 8-unit (14-unit) chain. Sketches of the B3LYP/6-31G* normal modes for the 14-unit chain can be found in the Supporting Information (Table S1–S3). Within a band, the intensity is not distributed uniformly, as illustrated by the IR and VCD intensities of the 14-unit oligomer (listed in Table S4 in the Supporting Information); the analysis is therefore performed by resorting to the localized-mode approach, as introduced by Jacob and Reiher.[22] The

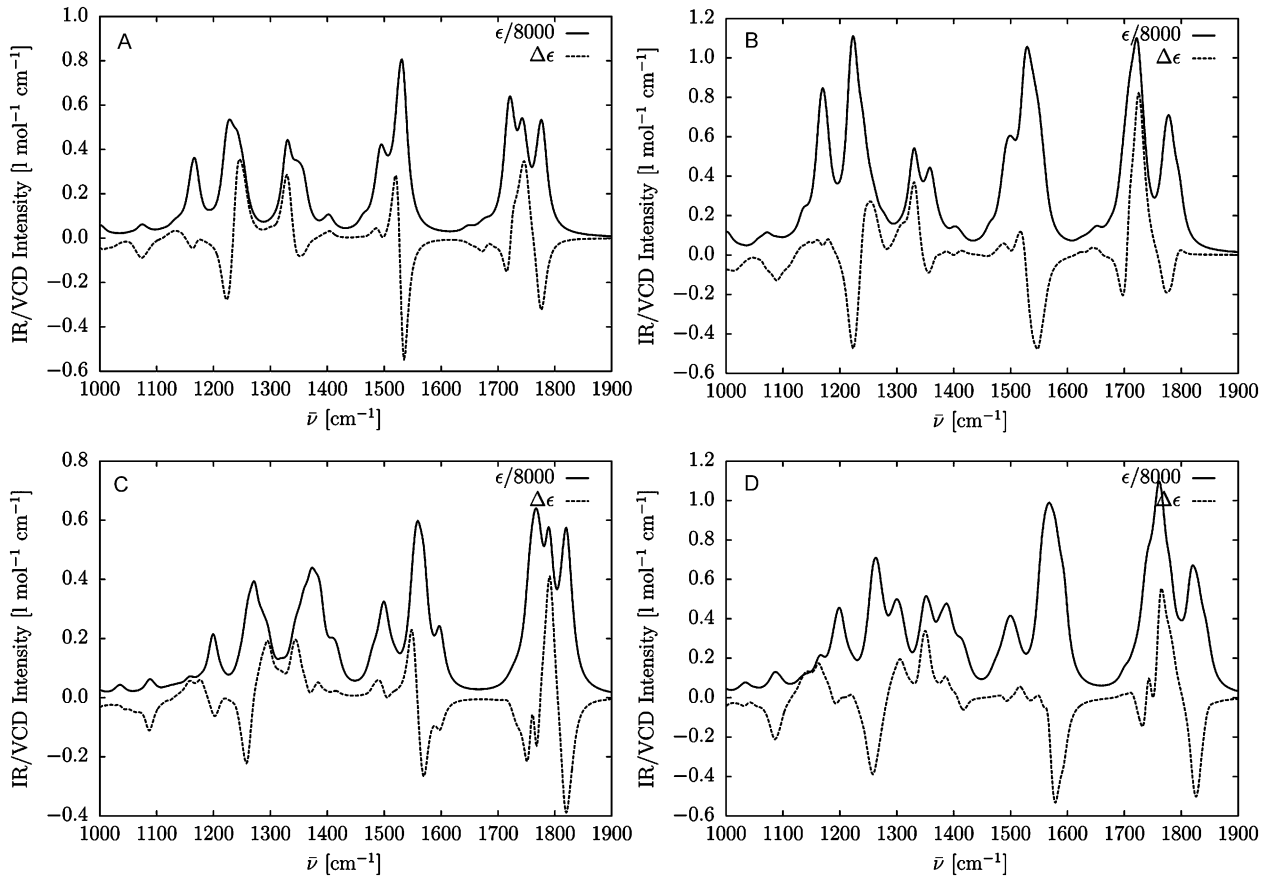

Figure 3. Simulated B3LYP/6-31G* A) 8-unit chain, and B) 14-unit chain and ωB97X-D/6-31G*, C) 8-unit chain, and D) 14-unit chain VCD (dotted line) and IR absorbance (ε/8000, black line) spectra of **1b**. Each transition is represented by a Lorentzian function with a full width at half maximum of 20 cm^{-1}. A multiplicative factor of 0.98 was used to scale the vibrational frequencies.

IR and VCD intensities associated with the localized modes are given in Table S4 and a typical localized mode for each of the three regions is sketched in Figure S4, both in the Supporting Information. For the amide II band, the total VCD intensity is negative ($-171.4\,m mol^{-1}$), as are the intensities of the majority of the localized modes (with the exception of two localized modes). The presence of positive VCD peaks close to 1520 cm^{-1} is explained as resulting from the coupling between the localized modes. The amide I band presents a positive total VCD intensity ($230.0\,m mol^{-1}$) and most of the localized modes have a positive VCD intensity. For the band associated with the C=O stretching of the ester groups, the total VCD intensity is negative ($-72.1\,m mol^{-1}$), but it is more than two times smaller in amplitude than the first band. The VCD intensities associated with the localized modes are less uniform than for the other two bands (with six modes having a positive VCD intensity).

At lower frequencies, two signatures are observed. The first one covers the 1210–1280 cm^{-1} range and consists of a negative peak followed by a positive one, whereas the second signature, in the 1290–1380 cm^{-1} zone, is made up of two positive peaks followed by a negative one. The atomic displacements giving rise to the first signature are of two types (Figure S5 in the Supporting Information): N–H bending and C–C(O) stretching associated with the positive band (type a) and C^{α}–H bending and C–O stretching associated with the negative peak (type b). For the second region, from 1290–1380 cm^{-1}, we observe four types of atomic displacements, all involving C^{α}–H wagging and bending of the methyl group attached to the C^{α} atom (Figure S5 in the Supporting Information). Type a′/c′ is described by bending motions of the Me group on the second/first (outer/inner) C^{α} atom coupled with the C^{α}–H wagging displacements in the direction toward the methyl group. Type b′/d′ is similar to type a′/c′ with the exception that the C^{α}–H wagging goes perpendicular. Within the 1290–1380 cm^{-1} region, the normal modes at low wavenumber are mainly of type c′ and have very weak VCD intensities. In the middle of that region, modes of types a′ and b′ give rise to two positive peaks, whereas the negative peak at higher wavenumbers originates from type d′ modes.

In a subsequent step, we checked the influence of different conformations on the VCD signatures. In the 14-unit LD-PIAA oligomer, the 11 torsion angles of the chain backbone plus the 14×6 torsion angles of the side arms completely define its structure. Nevertheless, in each side arm, only four out of the six torsion angles can move freely, because the torsion angles along the CO–NH and CO–OCH_3 bonds must be close to 180° owing to the N and O lone-pair delocalization towards the electron-acceptor C=O group. The torsion angles of the 14 lateral groups in the 14-unit LD-PIAA oligomer, optimized at the B3LYP/6-31G* level of theory, are listed in Table S5 in the Supporting Information. Besides the approximately 4_1 conformation of the polymer studied above, two other conformations (that is, TTTTTT and T0TTTT, in which T (trans) = 180°, and 0 (planar) = 0°; see below) of the 14-unit LD-PIAA oligomer have also been studied. In these conformations, prior to geometry optimization, the β-sheet structure of the initial 4_1 conformation is interrupted, that is, the 6 torsion angles of each of the 14 lateral groups are all forced to be equal to 180°, 180°, 180°, 180°, 180°, and 180° (conformer TTTTTT) or 180°, 0°, 180°, 180°, 180°, and 180° (conformer T0TTTT), in which the torsion angles are given consecutively from the N atom attached to the backbone to the OCH_3 extremity of the chain. The torsion angles of the chain backbone were set to 60° in accordance with the approximately 4_1 structure. From this starting point, the geometries were fully optimized at the B3LYP/6-31G* level of theory. The resulting torsion angles for the 14 lateral chains are given in Tables S6 and S7 in the Supporting Information. The backbone torsion angles of the TTTTTT and T0TTTT conformers, as well as the previous conformer, are given in Table S8 in the Supporting Information, together with their B3LYP/6-31G* energies. The calculations confirm the stability of the conformer displaying a β-sheet structure with hydrogen bonding between the amide side groups (Figure 4). In addition, the calculations show that: 1) the most stable structure is less compact with a distance between the first and the last backbone C atoms of 14.2 Å, versus 11.4 and 12.0 Å for the TTTTTT and T0TTTT conformers, respectively (Figure 4), 2) the approximately 4_1 helix consistently transforms into an approximate-

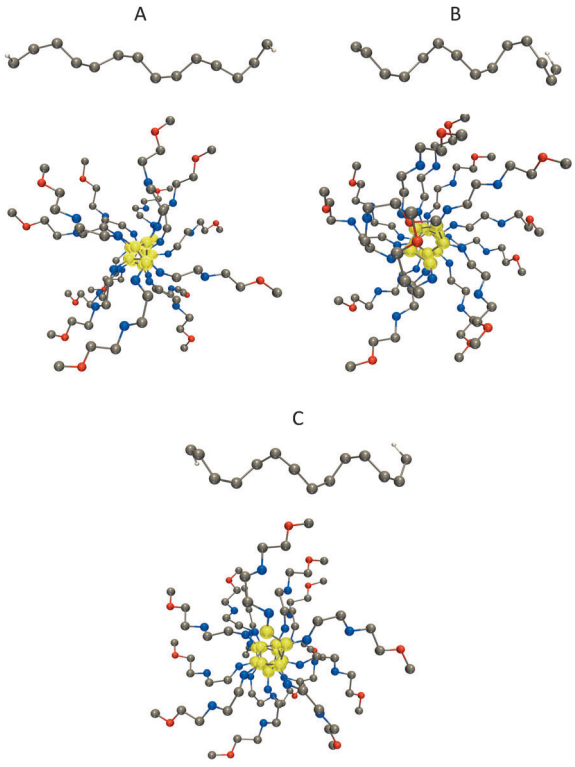

Figure 4. Sketches of the backbones (top) and sketches of the backbone and lateral groups (bottom) of three conformers (A: the approximately 4_1 conformation; B: the TTTTTT conformer; C: the T0TTTT conformer) of the 14-unit LD-PIAA compound calculated at the B3LYP/6-31G* level of theory. The backbone atoms are highlighted in yellow.

ly 5_1 helix in the two new conformers, and 3) the number of hydrogen bonds between the lateral chains decreases from the β-sheet structure to the T0TTTT conformer and even more to the TTTTTT conformer, in parallel with an increase of relative energy and a decrease of the mean backbone torsion angle. Furthermore, the IR and VCD spectra of the TTTTTT and T0TTTT conformers of the 14-unit LD-PIAA oligomer (Figure S3 in the Supporting Information) are clearly different from the spectra of the most stable approximately 4_1 conformation, with the differences being more pronounced in the VCD spectrum, in which the peak signs are reversed although the helicity is unchanged and right handed.

In polyisocyanopeptides, each of the four rows of hydrogen-bonded peptide side chains can be regarded as a β sheet that runs along the polymer helical axis (see Figure 1B), and therefore, the overall arrangement of the polymer has a helical β-sheet-like organization. In comparison, in β-sheet helices found in nature, such as those found in the bacterial enzyme pectate lyase C[23] or in insect antifreeze proteins,[24] the β-sheet architecture is constructed from polypeptides that are coiled into a large helix, formed by stacks of β sheets separated by loops. The synthetic β-helical analogues therefore differ from naturally occurring helical β-sheet structures by the presence of a supporting covalent core that induces the helicity. To further investigate this difference, we compared the torsion angles obtained from the most stable 14-unit LD-PIAA oligomer (see above; Table S5 in the Supporting Information) and the torsion angles (φ and ψ) in the canonical β helix found in proteins and visualized these in a histogram (Figure 5A). Note that, because one set of torsion angles (φ and ψ) belongs to one C^α atom, we would have two sets of dihedral angles in our polyisocyanide, which contains two C^α atoms per peptide side chain. However, both the inner C^α atom and the outer C^α atom have different linkages, instead of the peptide linkages found in proteins: the inner C^α atom is connected to the N=C group and the outer C^α atom is connected to a C=O ester group (Figure 5B). We can thus only compare the ψ (N–C–C–N) torsion angle of the inner C^α atom and the φ (C–N–C–C) torsion angle of the outer C^α with the torsion angles found in canonical β helices (Columns 2 and 4 of Table S5 in the Supporting Information, and Figure 5). The histogram of the φ and ψ dihedral angles for the calculated LD-PIAA shows φ angles between −10 and −60° and ψ angles between 60 and 160°. These values differ substantially from those found in naturally occurring β helices (φ values between approximately −160 and −120° and ψ values between approximately 120 and 180°). This difference can be attributed to the fact that, in the synthetic polyisocyanopeptides, the β sheets are covalently attached to a polymer backbone and are therefore not as flat as their natural analogues; they can thus be regarded as β-sheet helices with a twist.

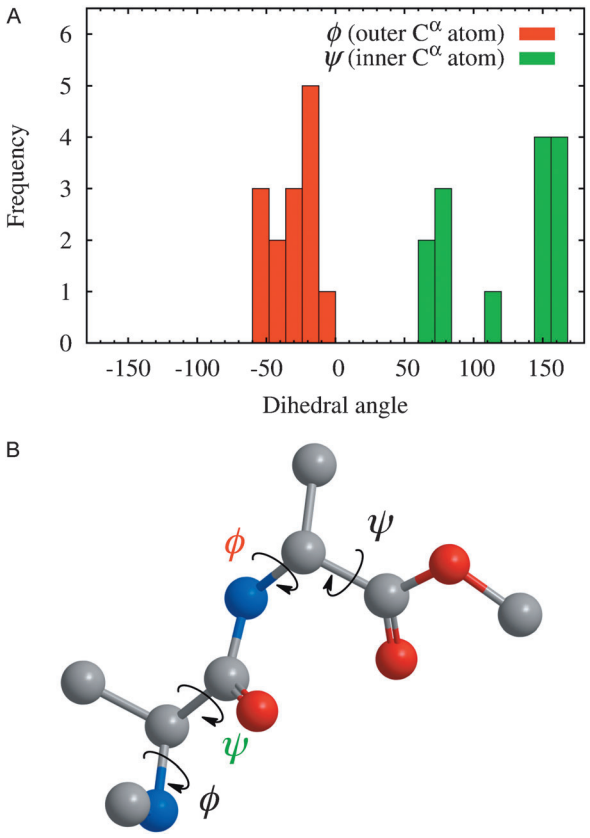

Figure 5. A) Histogram of the φ and ψ dihedral angles of the calculated LD-PIAA (14 units). B) Schematic drawing of the alanylalanine unit of the polymer (N→C direction) showing the φ and ψ angles used for the comparison with β helices found in nature.

Conclusion

In summary, ab initio calculations and VCD studies together provide a detailed and accurate description of the conformation of compounds **1**, which further adds to the current understanding of the architecture of biologically inspired polyisocyanides. The structure elucidation by using VCD spectroscopy and ab initio calculations presented here indicates that the polymerization of isocyanopeptides results in the formation of polymers that fold in a protein-like fashion to give helical fibers, in which the side chains are in a β-sheet-like arrangement. The torsion angles in the peptide chains of these synthetic polymers differ from those in their natural analogues because these chains are covalently attached to a polymer backbone. Finally, the VCD spectra allowed for a direct determination of the helical handedness of the polyisocyanopeptides by comparison of their C=N-stretching modes with the C=N-stretching mode of poly(isocyanooctane)s.

Experimental Section

General: Polymers DL-PIAA (**1a**) and LD-PIAA (**1b**) were synthesized according to literature procedures.[6] CD spectra were recorded on a

Jasco 810 UV/CD spectrometer equipped with a Peltier temperature control unit. The infrared and VCD spectra were recorded with a Bruker PMA 50 Tensor FTIR spectrometer. The light beam was collimated to the sample and passed through an optical filter (1800–600 cm^{-1}), a wired-grid polarizer, and a ZnSe 50 kHz photoelastic modulator (PEM; Hinds Instruments). The light was then focused by a ZnSe lens (10 cm focal length) onto a HgCdTe detector (Model D313/6) with BaF_2 windows. The PEM was adjusted for a maximum absorption at 1630 cm^{-1}. Calibration spectra were recorded by using a CdS multiple-wavelength plate and a second polarizer. The samples were held in a fixed pathlength of 0.1 mm between CaF_2 windows. The VCD spectra of **1** were recorded at a resolution of 4 cm^{-1}, by coadding scan times of 2×10, 40, and 60 min (total = 2 h, a 50:50 repartition of the two ten-minute experiments was used to average the data). To correct the VCD intensities for the racemic background, the average of the VCD intensities from both enantiomers was subtracted $\{I^{VCD}(\nu)=I^{VCD}(\nu)-0.5\times[I^{VCD,LD\text{-}PIAA}(\nu)+I^{VCD,DL\text{-}PIAA}(\nu)]\}$. The VCD spectra were obtained by making use of the VisualBasic PMA50 software, by using Blackman–Harris four-term apodization, Mertz phase correction, and a zero-filling factor of four.

Computational section: The conformation of the LD-PIAA polymer chain was obtained by modifying the side chains of the most stable structure of the polymer (an L-amino acid side chain), that we have previously reported.[5i] The extension of the side chains is expected to modify only marginally the hydrogen-bond network and, thus, the resulting helical structure. The polymer chain, which comprises 60 repeating units, was then optimized by molecular mechanics by using a modified version of the Dreiding force field adjusted against ab initio calculations of relevant torsion angles.[5i] In a second step, segments of 8 and 14 repeating units were extracted from that structure and further optimized at the DFT level by using the Gaussian 09 package.[21] Two exchange-correlation functionals were employed: B3LYP and ωB97X-D. The former is well known and well suited to compute vibrational spectra of molecules and polymers,[25] whereas the latter contains an additional term suitable for describing London dispersion forces, which could be important in these helical polymers that are structured by hydrogen bonds and other van der Waals forces. A 6-31G* basis set was chosen in order to provide accurate geometry and normal modes of vibration within an affordable CPU time. Its adequacy was checked by using the 6-311G* basis set. In addition, the impact of solvent ($CHCl_3$) effects was addressed by using the polarizable continuum model.[26] The vibrational frequencies and normal modes, as well as the atomic axial tensors (AAT) and atomic polar tensors (APT) were determined with the same level of theory by using Gaussian 09 as well. The IR and VCD intensities were then calculated by using a home-made program. A scaling factor of 0.98 was used to scale the vibrational frequencies and account for systematic overestimations due to missing anharmonic effects. Still DFT calculations are known to overestimate the frequency of the amide I band, whereas the uniform scaling procedure is reliable for the other bands. In the simulated spectra, each transition is represented by a Lorentzian function with a full width at half maximum (fwhm) of 20 cm^{-1}. The vibrational normal modes have been analyzed by employing the localized-mode procedure,[22,27] which consists of applying a unitary transformation to the normal modes of one band by maximizing a localization criterion, which allows specific couplings between the modes to be highlighted.

Acknowledgements

The Technology Foundation STW, NanoNed, NanoNextNL, the Council for the Chemical Sciences of The Netherlands Organisation for Scientific Research (CW-NWO), the Royal Netherlands Academy of Sciences, and the Ministry of Education, Culture and Science (Gravity program 024.001.035) are acknowledged for financial support. V.L. thanks the F.R.S.-FNRS for his Postdoctoral Researcher position. S.W. would like to acknowledge the European Research Council (ERC) for funding through grant no. 210999. This work is supported by the Belgian Government (IUAP no. P06-27 "Functional Supramolecular Systems"). The calculations were performed on the Interuniversity Scientific Computing Facility (ISCF) installed at the FUNDP, for which we gratefully acknowledge financial support from the F.R.S.-FRFC (Convention no. 2.4.617.07.F) and from the FUNDP. D.B. is a FNRS Research Director.

[1] *Foldamers: Structure, Properties, and Applications* (Eds.: S. Hecht, I. Huc), Wiley-VCH, Weinheim, **2007**.

[2] For reviews, see: a) J. J. L. M. Cornelissen, A. E. Rowan, R. J. M. Nolte, N. A. J. M. Sommerdijk, *Chem. Rev.* **2001**, *101*, 4039–4070; b) T. Nakano, Y. Okamoto, *Chem. Rev.* **2001**, *101*, 4013–4038; c) M. Suginome, Y. Ito, *Adv. Polym. Sci.* **2004**, *171*, 77–136; d) E. Yashima, K. Maeda, H. Iida, Y. Furusho, K. Nagai, *Chem. Rev.* **2009**, *109*, 6102–6211; e) J. G. Kennemur, B. M. Novak, *Polymer* **2011**, *52*, 1693–1710; f) J. G. Kennemur, B. M. Novak, *Isr. J. Chem.* **2011**, *51*, 1041–1051.

[3] For reviews, see: a) F. Millich, *Chem. Rev.* **1972**, *72*, 101–113; b) R. J. M. Nolte, *Chem. Soc. Rev.* **1994**, *23*, 11–19; c) E. Schwartz, M. Koepf, H. J. Kitto, R. J. M. Nolte, A. E. Rowan, *Polym. Chem.* **2011**, *2*, 33–47.

[4] R. J. M. Nolte, A. J. M. Van Beijnen, W. Drenth, *J. Am. Chem. Soc.* **1974**, *96*, 5932–5933.

[5] For some recent examples, see: a) N. Hida, F. Takei, K. Onitsuka, K. Shiga, S. Asaoka, T. Iyoda, S. Takahashi, *Angew. Chem.* **2003**, *115*, 4485–4488; *Angew. Chem. Int. Ed.* **2003**, *42*, 4349–4352; b) D. B. Amabilino, J. L. Serrano, J. Veciana, *Chem. Commun.* **2005**, 322–324; c) T. Kajitani, K. Okoshi, S. I. Sakurai, J. Kumaki, E. Yashima, *J. Am. Chem. Soc.* **2006**, *128*, 708–709; d) E. Schwartz, H. J. Kitto, R. de Gelder, R. J. M. Nolte, A. E. Rowan, J. Cornelissen, *J. Mater. Chem.* **2007**, *17*, 1876–1884; e) K. Okoshi, K. Nagai, T. Kajitani, S. I. Sakurai, E. Yashima, *Macromolecules* **2008**, *41*, 7752–7754; f) H. Onouchi, K. Okoshi, T. Kajitani, S. I. Sakurai, K. Nagai, J. Kumaki, K. Onitsuka, E. Yashima, *J. Am. Chem. Soc.* **2008**, *130*, 229–236; g) V. Palermo, M. B. J. Otten, A. Liscio, E. Schwartz, P. A. J. de Witte, M. A. Castriciano, M. M. Wienk, F. Nolde, G. De Luca, J. J. L. M. Cornelissen, R. A. J. Janssen, K. Muellen, A. E. Rowan, R. J. M. Nolte, P. Samori, *J. Am. Chem. Soc.* **2008**, *130*, 14605–14614; h) T. Kajitani, H. Z. Lin, K. Nagai, K. Okoshi, H. Onouchi, E. Yashima, *Macromolecules* **2009**, *42*, 560–567; i) E. Schwartz, V. Palermo, C. E. Finlayson, Y. S. Huang, M. B. L. Otten, A. Liscio, S. Trapani, I. Gonzalez-Valls, P. Brocorens, J. Cornelissen, K. Peneva, K. Mullen, F. C. Spano, A. Yartsev, S. Westenhoff, R. H. Friend, D. Beljonne, R. J. M. Nolte, P. Samori, A. E. Rowan, *Chem. Eur. J.* **2009**, *15*, 2536–2547; j) Z. Q. Wu, K. Nagai, M. Banno, K. Okoshi, K. Onitsuka, E. Yashima, *J. Am. Chem. Soc.* **2009**, *131*, 6708–6718; k) M. Banno, Z. Q. Wu, K. Nagai, S. Sakurai, K. Okoshi, E. Yashima, *Macromolecules* **2010**, *43*, 6553–6561; l) J. Kumaki, T. Kajitani, K. Nagai, K. Okoshi, E. Yashima, *J. Am. Chem. Soc.* **2010**, *132*, 5604–5606; m) V. Palermo, E. Schwartz, C. E. Finlayson, A. Liscio, M. B. J. Otten, S. Trapani, K. Muellen, D. Beljonne, R. H. Friend, R. J. M. Nolte, A. E. Rowan, P. Samori, *Adv. Mater.* **2010**, *22*, E81–E88; n) T. Kajitani, H. Onouchi, S. Sakurai, K. Nagai, K. Okoshi, K. Onitsuka, E. Yashima, *J. Am. Chem. Soc.* **2011**, *133*, 9156–9159; o) K. Tamura, T. Miyabe, H. Iida, E. Yashima, *Polym. Chem.* **2011**, *2*, 91–98.

[6] J. J. L. M. Cornelissen, W. S. Graswinckel, P. J. H. M. Adams, G. H. Nachtegaal, A. P. M. Kentgens, N. A. J. M. Sommerdijk, R. J. M. Nolte, *J. Polym. Sci. Part A* **2001**, *39*, 4255–4264.

[7] P. Samorí, C. Ecker, I. Gossl, P. A. J. de Witte, J. J. L. M. Cornelissen, G. A. Metselaar, M. B. J. Otten, A. E. Rowan, R. J. M. Nolte, J. P. Rabe, *Macromolecules* **2002**, *35*, 5290–5294.

[8] J. J. L. M. Cornelissen, J. J. J. M. Donners, R. de Gelder, W. S. Graswinckel, G. A. Metselaar, A. E. Rowan, N. A. J. M. Sommerdijk, R. J. M. Nolte, *Science* **2001**, *293*, 676–680.

[9] a) J. J. L. M. Cornelissen, N. A. J. M. Sommerdijk, R. J. M. Nolte, *Macromol. Chem. Phys.* **2002**, *203*, 1625–1630; b) J. J. L. M. Cornelissen, W. S. Graswinckel, A. E. Rowan, N. A. J. M. Sommerdijk, R. J. M. Nolte, *J. Polym. Sci. Part A* **2003**, *41*, 1725–1736; c) P. Bodis, E. Schwartz, M. Koepf, J. J. L. M. Cornelissen, A. E. Rowan,

R. J. M. Nolte, S. Woutersen, *J. Chem. Phys.* **2009**, *131*; d) C. M. Gowda, E. R. H. van Eck, A. M. van Buul, E. Schwartz, G. W. P. van Pruissen, J. J. L. M. Cornelissen, A. E. Rowan, R. J. M. Nolte, A. P. M. Kentgens, *Macromolecules* **2012**, *45*, 2209–2218.

[10] L. A. Nafie, T. A. Keiderling, P. J. Stephens, *J. Am. Chem. Soc.* **1976**, *98*, 2715–2723.

[11] a) T. B. Freedman, X. L. Cao, R. K. Dukor, L. A. Nafie, *Chirality* **2003**, *15*, 743–758; b) D. Dunmire, T. B. Freedman, A. A. Nafie, C. Aeschlimann, J. G. Gerber, J. Gal, *Chirality* **2005**, *17*, S101–S108; c) K. Monde, N. Miura, M. Hashimoto, T. Taniguchi, T. Inabe, *J. Am. Chem. Soc.* **2006**, *128*, 6000–6001; d) G. Tarczay, G. Magyarfalvi, E. Vass, *Angew. Chem.* **2006**, *118*, 1807–1809; *Angew. Chem. Int. Ed.* **2006**, *45*, 1775–1777; e) P. J. Stephens, F. J. Devlin, J. J. Pan, *Chirality* **2008**, *20*, 643–663; f) P. J. Stephens, F. J. Devlin, S. Schurch, J. Hulliger, *Theor. Chem. Acc.* **2008**, *119*, 19–28.

[12] a) P. Bour, T. A. Keiderling, *J. Am. Chem. Soc.* **1993**, *115*, 9602–9607; b) G. Yoder, T. A. Keiderling, F. Formaggio, M. Crisma, C. Toniolo, J. Kamphuis, *Tetrahedron: Asymmetry* **1995**, *6*, 687–690; c) T. A. Keiderling, R. A. G. D. Silva, G. Yoder, R. K. Dukor, *Bioorg. Med. Chem.* **1999**, *7*, 133–141; d) K. K. Lee, K. I. Oh, H. Lee, C. Joo, H. Han, M. Cho, *ChemPhysChem* **2007**, *8*, 2218–2226; e) E. Deplazes, W. van Bronswijk, F. Zhu, L. D. Barron, S. Ma, L. A. Nafie, K. J. Jalkanen, *Theor. Chem. Acc.* **2008**, *119*, 155–176; f) K. J. Jalkanen, I. M. Degtyarenko, R. M. Nieminen, X. Cao, L. A. Nafie, F. Zhu, L. D. Barron, *Theor. Chem. Acc.* **2008**, *119*, 191–210; g) A. Moretto, F. Formaggio, B. Kaptein, Q. B. Broxterman, L. Wu, T. A. Keiderling, C. Toniolo, *Biopolymers* **2008**, *90*, 567–574.

[13] a) T. A. Keiderling, *Curr. Opin. Chem. Biol.* **2002**, *6*, 682–688; b) D. Tsankov, B. Kalisch, J. H. Van de Sande, H. Wieser, *Biopolymers* **2003**, *72*, 490–499; c) G. Shanmugam, P. L. Polavarapu, *J. Am. Chem. Soc.* **2004**, *126*, 10292–10295; d) A. T. Krummel, M. T. Zanni, *J. Phys. Chem. B* **2006**, *110*, 24720–24727; e) S. L. Ma, X. L. Cao, M. Mak, A. Sadik, C. Walkner, T. B. Freedman, I. K. Lednev, R. K. Dukor, L. A. Nafie, *J. Am. Chem. Soc.* **2007**, *129*, 12364–12365.

[14] a) T. Buffeteau, L. Ducasse, L. Poniman, N. Delsuc, I. Huc, *Chem. Commun.* **2006**, 2714–2716; b) L. Ducasse, F. Castet, A. Fritsch, I. Huc, T. Buffeteau, *J. Phys. Chem. A* **2007**, *111*, 5092–5098.

[15] a) M. Urbanová, V. Setnicka, F. J. Devlin, P. J. Stephens, *J. Am. Chem. Soc.* **2005**, *127*, 6700–6711; b) H. Izumi, A. Ogata, L. A. Nafie, R. K. Dukor, *J. Org. Chem.* **2008**, *73*, 2367–2372; c) M. M. J. Smulders, T. Buffeteau, D. Cavagnat, M. Wolffs, A. P. H. J. Schenning, E. W. Meijer, *Chirality* **2008**, *20*, 1016–1022.

[16] a) T. Brotin, D. Cavagnat, J. P. Dutasta, T. Buffeteau, *J. Am. Chem. Soc.* **2006**, *128*, 5533–5540; b) C. Gautier, T. Burgi, *J. Am. Chem. Soc.* **2006**, *128*, 11079–11087; c) C. Johannessen, P. W. Thulstrup, *Dalton Trans.* **2007**, 1028–1033; d) A. G. Petrovic, P. L. Polavarapu, *J. Phys. Chem. A* **2007**, *111*, 10938–10943.

[17] a) V. Andrushchenko, J. L. McCann, J. H. van de Sande, H. Wieser, *Vib. Spectrosc.* **2000**, *22*, 101–109; b) F. Wang, P. L. Polavarapu, F. Lebon, G. Longhi, S. Abbate, M. Catellani, *J. Phys. Chem. A* **2002**, *106*, 5918–5923; c) H. Z. Tang, E. R. Garland, B. M. Novak, J. T. He, P. L. Polavarapu, F. C. Sun, S. S. Sheiko, *Macromolecules* **2007**, *40*, 3575–3580; d) T. Kawauchi, A. Kitaura, J. Kumaki, H. Kusanagi, E. Yashima, *J. Am. Chem. Soc.* **2008**, *130*, 11889–11891; e) M. Kudo, T. Hanashima, A. Muranaka, H. Sato, M. Uchiyama, I. Azumaya, T. Hirano, H. Kagechika, A. Tanatani, *J. Org. Chem.* **2009**, *74*, 8154–8163; f) C. Merten, A. Hartwig, *Macromolecules* **2010**, *43*, 8373–8378.

[18] R. Schweitzer-Stenner, *J. Phys. Chem. B* **2012**, *116*, 4141–4153.

[19] J. J. L. M. Cornelissen, *Pure Appl. Chem.* **2002**, *74*, 2021–2030.

[20] E. Schwartz, S. R. Domingos, A. Vdovin, M. Koepf, W. J. Buma, J. J. L. M. Cornelissen, A. E. Rowan, R. J. M. Nolte, S. Woutersen, *Macromolecules* **2010**, *43*, 7931–7935.

[21] Gaussian 09, Revision A02, M. J. Frisch, G. W. Trucks, H. B. Schlegel, G. E. Scuseria, M. A. Robb, J. R. Cheeseman, G. Scalmani, V. Barone, B. Mennucci, G. A. Petersson, H. Nakatsuji, M. Caricato, X. Li, H. P. Hratchian, A. F. Izmaylov, J. Bloino, G. Zheng, J. L. Sonnenberg, M. Hada, M. Ehara, K. Toyota, R. Fukuda, J. Hasegawa, M. Ishida, T. Nakajima, Y. Honda, O. Kitao, H. Nakai, T. Vreven, J. A. Montgomery, Jr., J. E. Peralta, F. Ogliaro, M. Bearpark, J. J. Heyd, E. Brothers, K. N. Kudin, V. N. Staroverov, R. Kobayashi, J. Normand, K. Raghavachari, A. Rendell, J. C. Burant, S. S. Iyengar, J. Tomasi, M. Cossi, N. Rega, J. M. Millam, M. Klene, J. E. Knox, J. B. Cross, V. Bakken, C. Adamo, J. Jaramillo, R. Gomperts, R. E. Stratmann, O. Yazyev, A. J. Austin, R. Cammi, C. Pomelli, J. W. Ochterski, R. L. Martin, K. Morokuma, V. G. Zakrzewski, G. A. Voth, P. Salvador, J. J. Dannenberg, S. Dapprich, A. D. Daniels, Ö. Farkas, J. B. Foresman, J. V. Ortiz, J. Cioslowski, D. J. Fox, Gaussian, Inc., Wallingford, CT, **2009**.

[22] C. R. Jacob, M. Reiher, *J. Chem. Phys.* **2009**, *130*.

[23] M. D. Yoder, N. T. Keen, F. Jurnak, *Science* **1993**, *260*, 1503–1507.

[24] Y. C. Liou, A. Tocilj, P. L. Davies, Z. C. Jia, *Nature* **2000**, *406*, 322–324.

[25] X. Drooghaag, J. Marchand-Brynaert, B. Champagne, V. Liegeois, *J. Phys. Chem. B* **2010**, *114*, 11753–11760.

[26] J. Tomasi, R. Cammi, B. Mennucci, C. Cappelli, S. Corni, *Phys. Chem. Chem. Phys.* **2002**, *4*, 5697–5712.

[27] V. Liégeois, B. Champagne, *Theor. Chem. Acc.* **2012**, *131*, 1–15.

Received: January 8, 2013
Revised: May 7, 2013
Published online: August 12, 2013

